LAWRENCE
LIVERMORE
NATIONAL
LABORATORY

LLNL-JRNL-822417

The bands method for tabulating NLTE material properties

Y. Frank, H. A. Scott

May 10, 2021

High Energy Density Physics

Disclaimer

The bands method for tabulating NLTE material properties

Yechiel Frank[1] and Howard A Scott[1,*]

[1]*Lawrence Livermore National Laboratory, 7000 East Ave. Livermore CA 94550*

The use of Non-Local Thermal Equilibrium (NLTE) material properties within radiation-hydrodynamic simulations remains a major challenge. The plasma radiative and EOS properties in NLTE can depend on the detailed local radiation field and electron energy distribution. Fully characterizing each of these quantities may require 10's to 100's of parameters, making tabulation effectively impossible and requiring expensive calculations for each set of conditions within the simulation. In this work we present a new method that characterizes the local radiation field with a limited number of parameters. This permits pre-calculation and tabulation of the material properties, allowing codes to perform NLTE radiation-hydrodynamic simulations which would otherwise be computationally prohibitive.

* hascott@llnl.gov

I. INTRODUCTION

Non-local thermodynamic equilibrium (NLTE) radiative processes, such as emission and absorption of radiation, play an important role in studying a wide range of laboratory and astrophysical plasmas [1]. Collisional-radiative (CR) models to simulate and analyze spectra produced by plasmas in NLTE have been developed over many years [2]. In recent years vast progress has been made in the development of new laboratory plasma sources, from the National Ignition Facility (NIF) to the Extreme Light Infrastructure project (ELI), powerful Z-pinch machines and X-ray free electron lasers. Alongside with this experimental developments there has also been significant advancement in NLTE modeling, both theoretically and computationally, for example, in a series of NLTE code-comparison workshops (e.g. [3, 4]).

The main challenge in modeling NLTE plasmas is that the number of population levels that can be calculated with even modern machines is not much larger than $\sim 10^6$ levels [5]. However, for many applications in medium to high Z hot plasmas, even this number is not sufficient. In these cases, the computing power required for detailed level accounting calculations is overwhelming. Therefore, models that take into account average atomic quantities are commonly used for practical calculations. This problem becomes more pressing when one needs to use these atomic calculations in radiation-hydrodynamic simulations. In these simulations the radiative properties of plasmas over a very large range of different conditions is required. These radiative properties are needed for each hydrodynamic cell at each time-step of the simulation, creating a huge computational load if the properties must be recalculated each time.

For plasmas under LTE conditions the use of pre-calculated tabulated data is straightforward as the plasma can be fully characterized by its density and temperature. The data can be stored in a simple two dimensional table for interpolation at any temperature and density needed by the hydrodynamic simulation. For NLTE plasmas on the other hand, the radiative properties of the plasma can depend on the detailed local radiation field and electron energy distribution. Each of these quantities may require 10's to 100's of parameters to be fully characterized making pre-calculation and tabulation prohibitive. Therefore, the most reliable way for obtaining NLTE atomic properties in radiation-hydrodynamic simulations is to perform the CR calculation inline, calculating plasma properties at each time step for each hydrodynamic cell. This results in a very high computational load. The NLTE calculations can easily become the most time consuming element of the total simulation [6, 7]. Moreover, in order to perform these atomic calculations inline one needs to use a highly averaged model which reduces the model's accuracy. Methods for reducing the calculational time or tabulating the NLTE radiative properties have been recently proposed [5, 8, 9].

In this work we present a new method which allows tabulation of radiative properties by describing the local radiation field using a very limited number of parameters. The method utilizes the active atomic shells of each element to identify the most important spectral ranges, denoted as bands. It then uses the radiative intensity only in these bands for the atomic calculation. The method focuses on radiation in those frequency intervals which interact most strongly with the material, with the intervals obtained from material properties in the absence of radiation. This should adequately capture the effects of the radiation on the material properties so long as significant radiation is not trapped in the frequency intervals which are neglected. We find this manner of characterizing the radiation to be a sufficient approximation in many cases for radiation-hydrodynamic simulations. The method still assumes a thermal distribution for the free electrons which is valid in many applications.

The bands method is presented here for use within radiation-hydrodynamic simulations. The spectral accuracy required within the framework of these simulations differs from the requirements for detailed spectroscopic analysis. Radiation-hydrodynamic simulations regularly use 100-200 radiation groups to characterize the local radiation field in each simulation cell, while spectroscopic analysis often requires a much higher level of spectral details and accuracy. The bands method is intended to be an approximate method accurate enough for use in radiation-hydrodynamic simulations.

This paper is organized in the following way: In Sec. II the computational cycle of radiation-hydrodynamic simulations is presented to explain the challenges inherent in performing a simulation in a consistent way under NLTE conditions. In Sec. III the different steps of the proposed bands method are described and demonstrated. Sec. IV presents a set of examples comparing the bands method to inline calculations to demonstrate the method's validity over a wide range of conditions. In Sec. V we discuss tabulating and interpolating data in the bands method. Finally, we summarize our findings in Sec. VI.

II. PROBLEM DEFINITION AND CURRENT APPROACHES

In order to better understand the scope in which the method presented in this work is intended to be used, it is important to first describe the the workflow of radiation-hydrodynamic simulations. This workflow is presented in Fig. 1, which schematically depicts three computational processes critical to both LTE and NLTE simulations: the hydrodynamic model, the atomic model and the radiation transfer model.

The first part is the hydrodynamic model. In this part the set of equations describing the motion of a fluid is solved. In order to calculate the energy density and temperature at each location in the plasma the hydrodynamic model must include the energy flux and the equation of state (EOS) in each simulation cell. The energy flux itself can be the product of multiple physical processes. For laser produced plasma, the list includes laser absorption, electron transport and radiation transport as just a few examples. However, in the context of the current work we shall focus on the radiation flux only. Both the EOS and the radiation flux are dependent on the microscopic conditions of the plasma, the populations of different ionization and excitation levels of

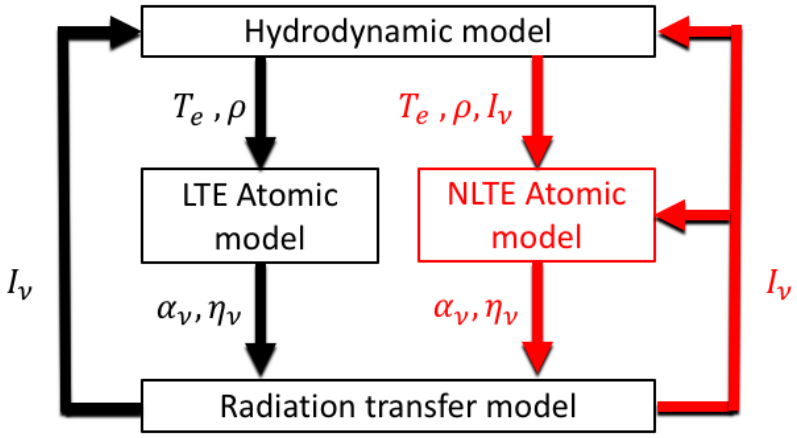

FIG. 1. (Color online) Schematic depiction of radiation-hydrodynamic simulations. On the left, in black, is the LTE case. On the right, in red, is the NLTE case.

the plasma.

The second part is the atomic model. In this part the microscopic conditions of the plasma are calculated. This calculation can be performed assuming LTE or by solving an NLTE model. The full description of the atomic models in LTE and NLTE are beyond the scope of this work. Details can be found in [2, 10] as two examples. The output of the atomic model is the plasma EOS and the radiative properties, opacity and emissivity, denoted by α_ν and η_ν respectively.

The third part is the radiation transfer model. In this part the transport of energy via radiation from one location in the plasma to another is calculated. The radiation transport model uses the radiative properties calculated by the atomic model to obtain the radiation intensity I_ν that can now be inserted again into the the hydrodynamic model to complete the cycle.

All three parts should be solved self-consistently. The equations describing the microscopic conditions should be solved together with the hydrodynamic equations and the radiation transfer. However, since solving all these equations together is computationally prohibitive, an operator splitting is commonly used. Each of the three parts is solved separately. This process should then be iterated to insure the convergence of the results.

As depicted in Fig. 1, under LTE conditions the above described algorithm serves as an adequate model for a calculational cycle, as the atomic model depends only on the temperature and density which are determined by the hydrodynamics and radiation transport (and other processes on the same timescale). It is also quite common to iterate between the temperature and intensity within the radiation transfer model with fixed opacity and an emissivity consistent with the LTE condition. Under NLTE conditions however, the local radiation field can affect the atomic calculation on much shorter timescales. In this case, the radiation transport model should be solved self-consistently with the atomic model, or at least one has to iterate over the smaller loop of the atomic and radiation transfer models to achieve convergence. This is depicted in Fig. 1 by the input of I_ν back into the atomic calculation. As stated in Sec. I current radiation-hydrodynamic codes calculate the NLTE atomic properties inline. In such a case iterating over this calculation can also make the simulation computationally prohibitive. Therefore, even advanced radiation-hydrodynamic codes use the same convergence scheme in NLTE as in LTE, with fixed opacity plus an assumed model for emissivity as a function of temperature.

To summarize, evaluating NLTE material properties inline in radiation-hydrodynamic codes compromises simulations in multiple ways.

1. Use of even the simplest highly-averaged atomic models presents a huge computational load.
2. Use of more accurate atomic models to better simulate the underlying physics is beyond current capabilities.
3. The computational cost discourages or prohibits iterating to self-consistently solve the atomic model with the radiation transport.

Being able to pre-calculate and tabulate NLTE atomic properties and use them in a simulation, similar to how LTE atomic properties are used, can solve the problems listed above. However, as mentioned in Sec. I, radiation-hydrodynamics codes use 100's of radiation energy groups to describe the local radiation field. Using the radiation groups as independent parameters, e.g. 102 parameters to characterize the plasma conditions - 100 for the radiation field plus electron temperature and density - is not feasible for this purpose. If one wishes to sample only 10 values for each parameter in the table, a total of 10^{102} calculations would be needed. Creating such a table is clearly not possible.

III. BANDS METHOD DESCRIPTION

In order to overcome the challenges presented in Sec. II we suggest the following approach:

1. For a set of given plasma conditions, calculate the ionization level and radiative properties with **NO** radiation field present.

2. Identify the active charge states, those which are populated or are connected to a populated charge state through ionization or recombination, either collisionally at the given temperature or radiatively with the anticipated radiation field.

3. Identify the active atomic shells, hose contributing the electrons participating in these transitions, and the corresponding photon frequency ranges (bands) that are expected to contribute to the radiative effects. We will denoted the shells with spectroscopic notation by the principal quantum number of the lower state electron, i.e. K-shell for n=1, L-shell for n=2, etc.

4. Calculate the EOS and radiative properties using a single averaged intensity value in each of the above identified bands. In most cases only 2 or 3 such bands will be needed for each plasma temperature and density. The results can than be pre-calculated and stored for future interpolation as functions of the temperature, density and average radiation intensity in the active bands.

It is best to explain the steps described above with an example. Consider a Cu plasma with electron temperature of $T_e = 1keV$, electron density of $N_e = 1e19cm^{-3}$ and a radiation field I_ν. Using the SEMILLAC code [11, 12], we first calculate the atomic properties without a radiation field. We obtain an average ionization for these plasma conditions of $Z^* = 24.6$. The charge state distribution shows non-negligible population in charge states from He-like to N-like, $Cu^{+27} - Cu^{+22}$, as presented in Fig. 2.

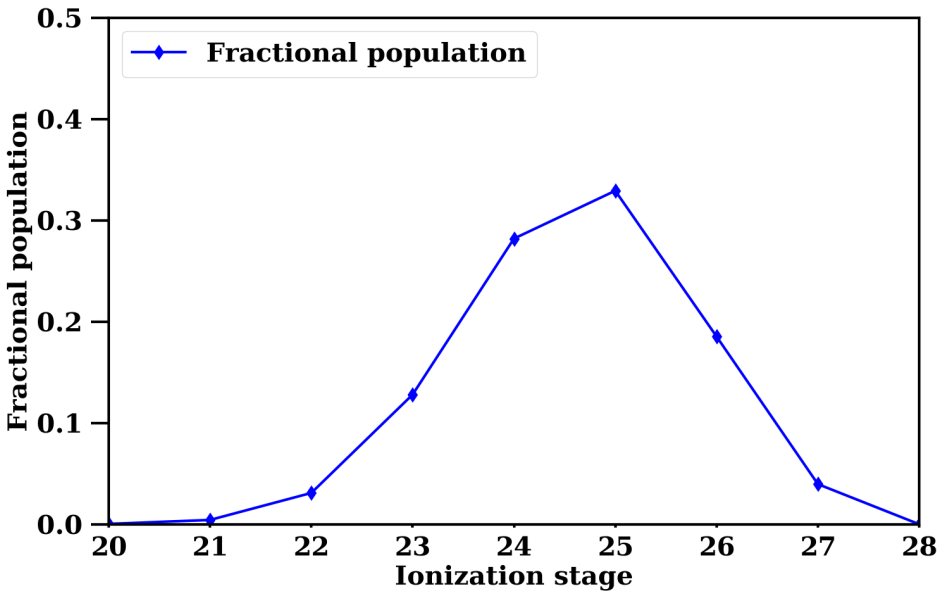

FIG. 2. (Color online) Fractional population of charge states for Cu plasma at $T_e = 1keV$ and $N_e = 1e19cm^{-3}$ with no radiation field.

The active shells in this case are the L-shell and the K-shell. For each shell the range of the photon band energies are determined by the lowest bound-bound (BB) transition energy from the ground state and the highest bound-free (BF) transition energy. For example, in the L-shell case the BB transition of lowest energy is the $2p - 3s$ transition in the N-like ion, while the BF transition of highest energy is for ionization of the ground state Li-like ion. Since BF transitions are not localized in energy, the upper energy of the band should be located some distance above the edge . We find that a 20% above the edge energy is a good choice for this factor. This choice is semi-empirical based on the comparison of the approximated simulations with detailed ones. The results of the bands method are not highly sensitive to the choice of this factor. Taking a much larger factor will result in lower average intensity in the entire band and therefore will reduce the accuracy of the results. Taking a very small factor close to 1 will result in neglecting an important section of the relevant band. The same process can be applied for the K-shell. The result in this case is that there are two photon energy bands that need to be taken into account: 1150-3300 eV for the L-shell and 8100-13300 eV for the K-shell. In order to calculate the EOS and radiative properties of plasma at the same temperature and density but for any given radiation field, only the the averaged intensities in these two bands will be used.

IV. COMPARISON OF DETAILED AND BANDS METHOD CALCULATIONS

After describing the bands method in Sec. III, we now look at several examples to demonstrate the validity of this method. For this comparison we shall compare the bands method results to those obtained with a radiation field described with a single parameter, the effective temperature. In this approach one derives a radiation temperature T_r based on the total radiative energy, regardless of the energy distribution, and assumes that the radiation field has a Planckian distribution at that temperature.

Let us look at a plasma with the same temperature and density as described in Sec. III, $T_e = 1keV$ and $N_e = 1e19cm^{-3}$, but now with a radiation field applied to the plasma.

The radiation field we apply first is a combination of two Planckians. The first is itself a thermal source while the second provides harder x-rays. Such radiation profiles can be found for example in the NIF hohlraum [13] experiments or in Z-pinch experiments where secondary radiation sources can be created from the infrastructure materials [14]. The radiation field used in the calculation is the sum of a 300 eV non-diluted Planckian and a 3000 eV Planckian with a dilution factor of 10^{-4}, as presented in Fig. 3.

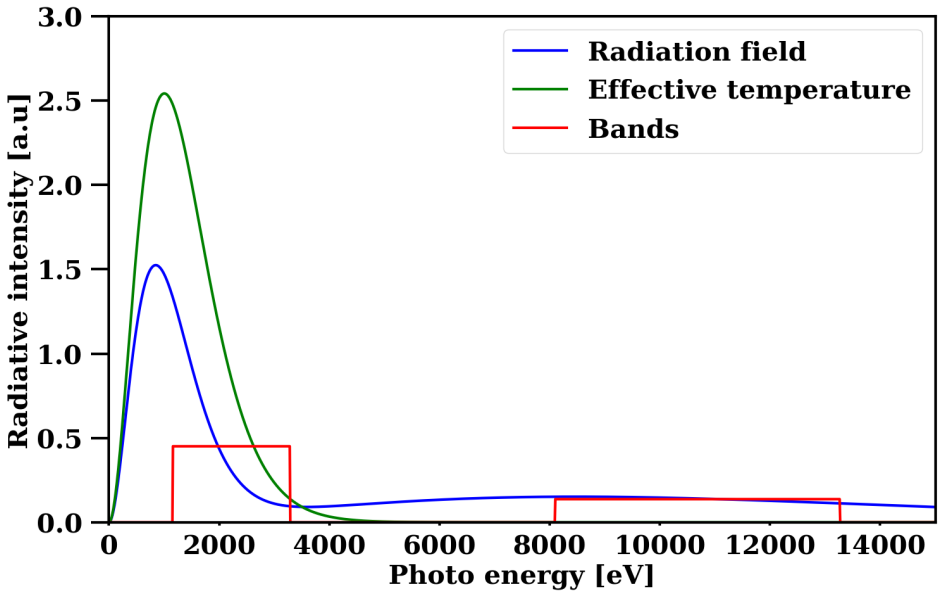

FIG. 3. (Color online) Radiation field for the first example. Blue: the full detailed radiation field of 300 eV Planckian and a 3000 eV Planckian with a dilution factor of 10^{-4}. Green: the effective temperature of 356 eV. Red: the bands method approximation for the radiation field.

In this case the average ionization obtained by the detailed calculation is $Z^* = 28.96$, the effective temperature treatment result is $Z^* = 27$, and the bands method result is $Z^* = 28.91$. The plasma absorption and emission coefficients for this case are presented in Figs. 4 and 5.

In this case it can be seen that the effective temperature treatment fails due to the lack of any hard X-ray portion of the radiation field. This results in a much lower average ionization as no K-shell electrons are ionized. In the emissivity, seen in Fig. 5, this appears as the lack of K-shell emission as K-shell electrons are not excited or ionized.

A second case we consider is taken from a radiation-hydrodynamic simulation. This case was taken from a 1D simulation of a laser of intensity $I = 1e14W/cm^2$ hitting a planar Cu foil. The simulation itself was done with a simple atomic model using SEMILLAC. We extract one set of conditions from the simulation and compare results from the different approaches. The plasma conditions in this example are $T_e = 1.54KeV$ and $N_e = 1.7e21cm^{-3}$. The radiation field taken from the simulation is presented by the blue curve in Fig. 6. In this case the radiation effective temperature is 213eV. However, the radiative energy distribution is far from being Planckian. The average ionization obtained in this case for the different treatments is $Z^* = 26.27$ with no radiation field, $Z^* = 26.6$ for the detailed calculation, $Z^* = 26.4$ for the effective temperature approach and $Z^* = 26.5$ using the bands method. The plasma absorption and emission for this case are presented in Figs. 7 and 8.

In this case the L-shell is almost completely ionized even without a radiation field. The radiation field effect is therefore seen mostly in the K-shell region at photon energies above 8000 eV. This effect is more prominent in the K-shell emissivity as no K-shell electrons are ionized or excited without radiation.

As a final example we look at a more extreme case of a lower density and lower temperature plasma driven by a radiation field with an effective temperature higher than the electron temperature. Such cases can be found for example in photoionizing plasma experiments [15]. The plasma conditions for this case are: $T_e = 100eV$ and $N_e = 1e17cm^{-3}$. The radiation field is now a combination of two diluted Planckians, a first Planckian at 400 eV multiplied by a factor of 1.3 and harder radiation in

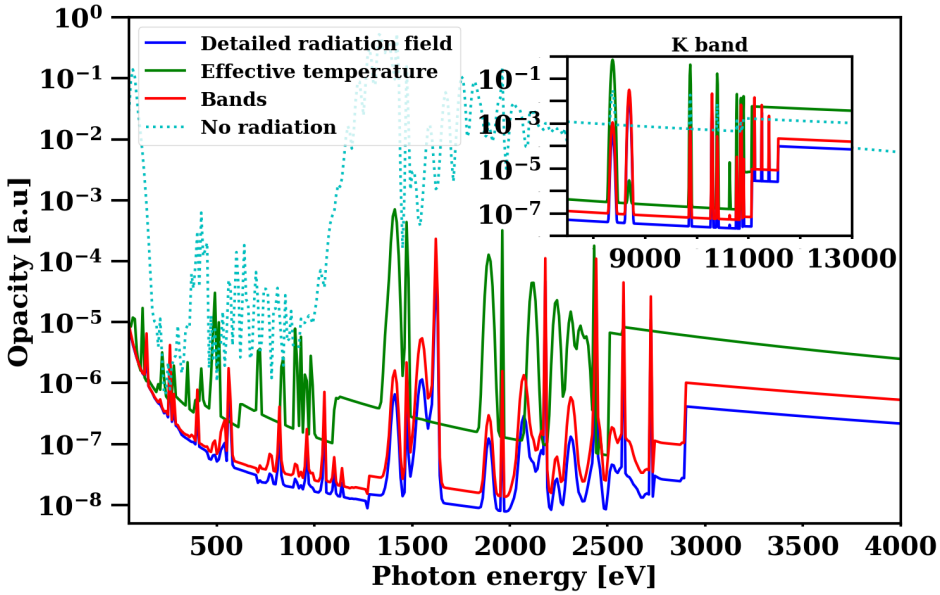

FIG. 4. (Color online) Plasma absorption coefficient for the first example. Blue: the full detailed radiation field. Green: the effective temperature of 356eV. Red: the bands method approximation for the radiation field. Dotted Cyan: no radiation field.

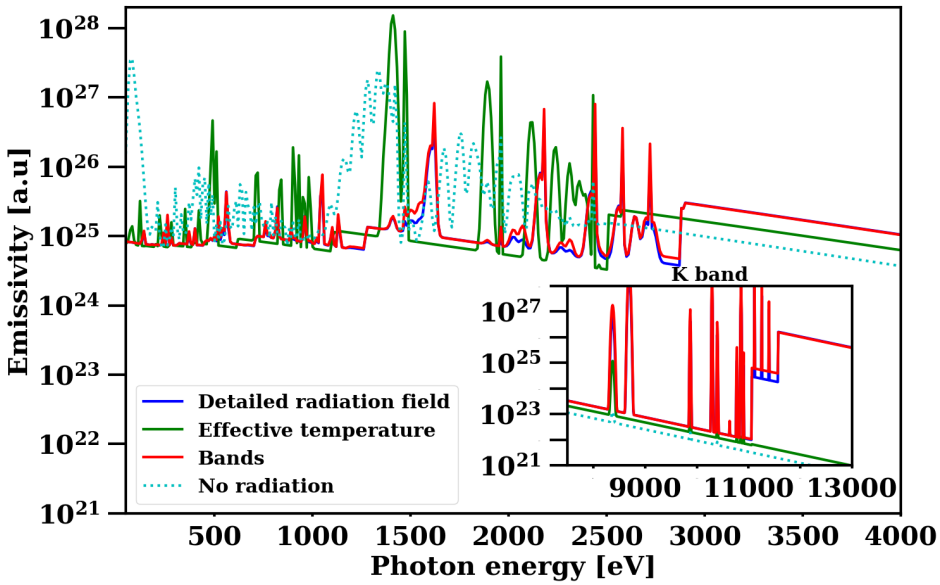

FIG. 5. (Color online) Plasma emissivity for the first example. Blue: the full detailed radiation field. Green: the effective temperature of 356eV. Red: the bands method approximation for the radiation field. Dotted Cyan: no radiation field.

the form of an 800 eV Planckian with a dilution factor of 10^{-4}. The radiation fields for the different approaches in this case are presented in Fig. 9.

As can be seen in Fig. 9 for this case, due to the lower electron temperature there are 3 active bands, the M, L and K bands. The figure also shows that in this case the effective temperature approximation is very close to the detailed radiation field for photon energies below 7 keV. The fractional populations of the different ionization stages in this case are presented in Fig. 10

In this case the radiation field shifts the average ionization by more than 10 charge states, implying that the radiation field is a dominant factor in this case.

We now turn to examine the absorption and emission coefficients in this case. These are presented in Figs. 11 and 12.

In this case, even more than in the first two, it is clear that totally neglecting the radiation field results in completely erroneous radiative properties. The effective temperature seems to be a better approximation than the bands method here. However, none of these approximate methods work well in this case as the radiation is the most important driver of the atomic system

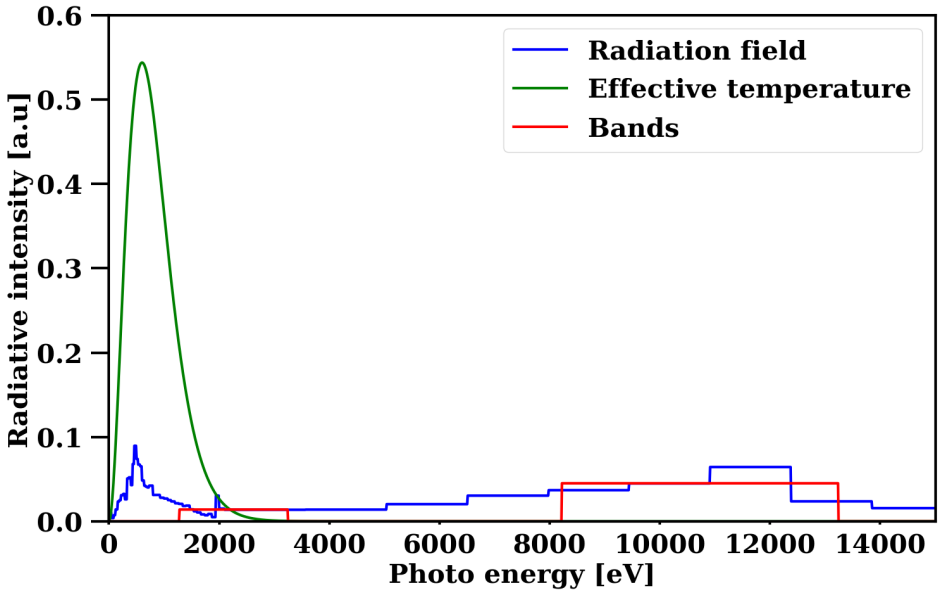

FIG. 6. (Color online) Radiation field for the second example. Blue: the full detailed radiation field taken from the radiation-hydrodynamic simulation. Green: the effective temperature treatment of 213 eV. Red: the bands method approximation for the radiation field.

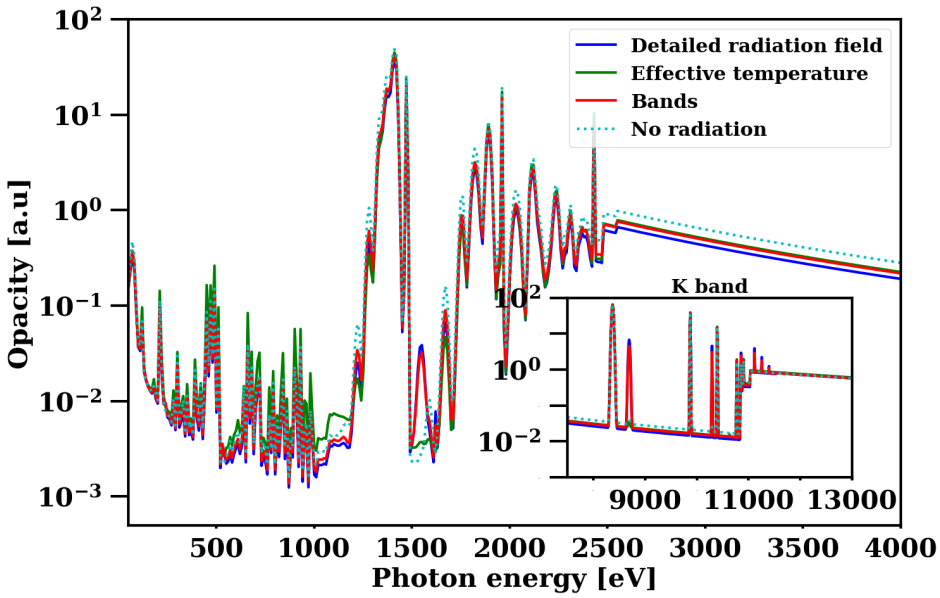

FIG. 7. (Color online) Plasma absorption for the second example case. Blue: using the full detailed radiation field. Green: using the effective temperature treatment of 312 eV Planckian. Red: using the bands method approximation for the radiation field. Dotted Cyan: with no radiation field.

in these conditions. The effective temperature and the band method produce a reasonable average ionization balance due to the system being mostly in He-like stage. The small fractional population of H-like ions seen in the detailed calculation is not reproduced using any of the approximate methods. This divergence leads to significant differences in the absorption and emission coefficients. In summary, in this case the use of the bands method is no longer valid, as expected since the radiation is the main driver of the system.

It is important to keep in mind that the method is intended as an approximation for use in radiation-hydrodynamic simulations. While in some cases a different approximation might provide better results, the advantage of this method is its applicability over a wide range of different conditions.

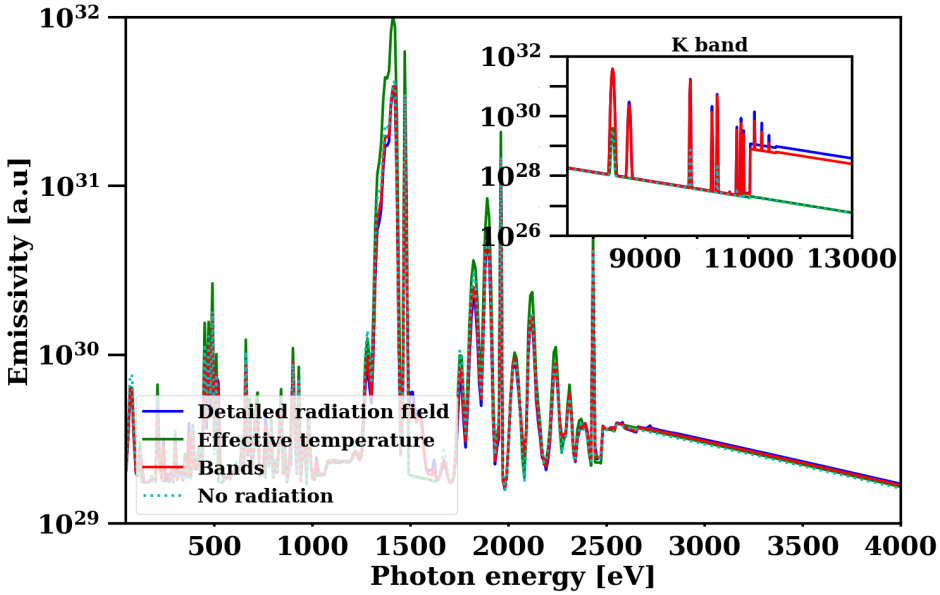

FIG. 8. (Color online) Plasma emissivity for the second example case. Blue: using the full detailed radiation field. Green: using the effective temperature treatment of 312 eV Planckian. Red: using the bands method approximation for the radiation field. Dotted Cyan: with no radiation field.

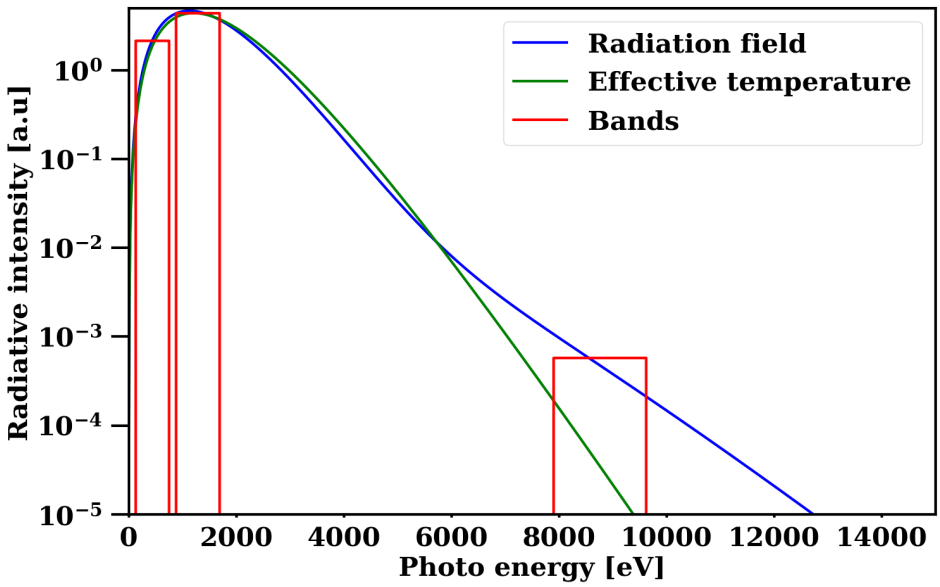

FIG. 9. (Color online) Radiation field for the third example. Blue: the full detailed radiation field. Green: the effective temperature of 428 eV. Red: the bands method approximation for the radiation field.

V. TABULATION AND INTERPOLATION

As discussed in Sec. II the goal of this method is to be useful for pre-calculating and tabulating atomic properties for use in radiation-hydrodynamic simulations. However, the tabulation appropriate for this method is somewhat different than that used in the LTE case or even for the effective temperature method. In these methods the atomic properties are tabulated over a fixed "square" grid of the relevant parameters. In the LTE case this is a two dimensional grid of temperature and density, while for the effective temperature method it is a three dimensional grid of temperature, density, and T_r. For the bands method the parameters describing the radiation field can vary with temperatures and densities. Therefore, interpolating between different points is not straightforward. We find the following algorithm to be practical and give good results. For a plasma at given conditions, T_e, n_e and I_ν:

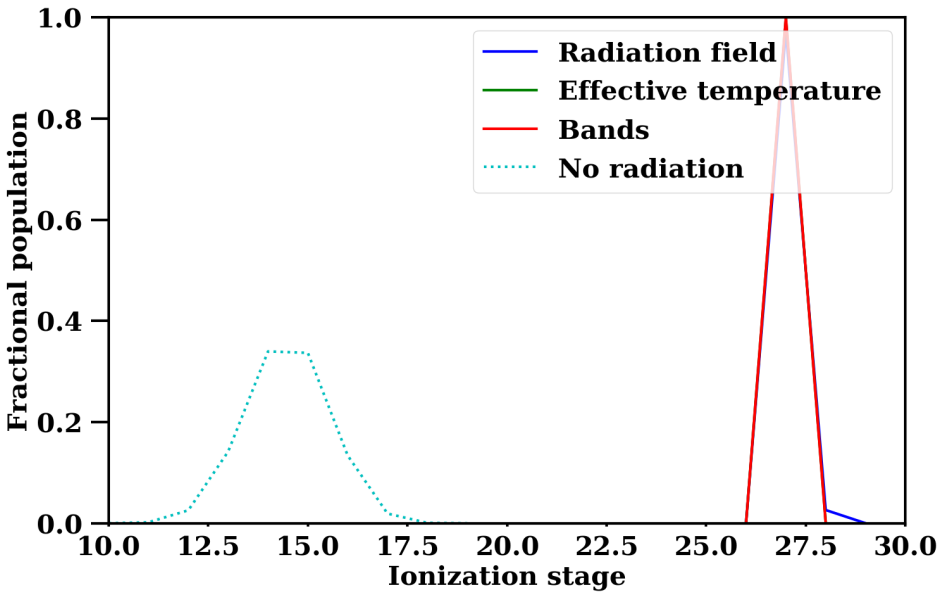

FIG. 10. (Color online) fractional populations of ionization stages for the third example. Blue: using the full detailed radiation field. Green: using the effective temperature of 428 eV. Red: using the bands method approximation for the radiation field. Dotted Cyan: with no radiation field.

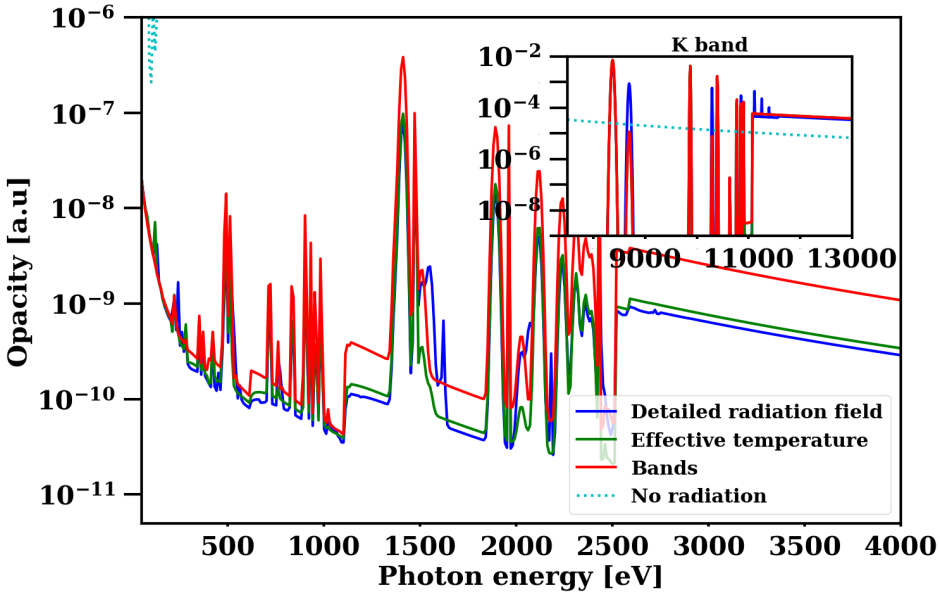

FIG. 11. (Color online) Plasma absorption for the third example. Blue: using the full detailed radiation field. Green: using the effective temperature of 428 eV. Red: using the bands method approximation for the radiation field. Dotted Cyan: with no radiation field.

- Locate the closest points in the table taking into account only the electron temperature and density. In the general case there are four such points.
- At each tabulated point average the detailed radiation field to the bands of that point and interpolate to get the radiative properties between the pre-calculated radiation intensity values. This results in the general case in four sets of opacities and emissivities, $\alpha_\nu(T_e, n_e)$, $\eta_\nu(T_e, n_e)$.
- Interpolate between the four sets to get the values for the desired value of T_e and n_e.

The choice of tabulation points can be dependent on the specific problem in hand, as is the resolution at which each parameter is sampled. The algorithm described above is consistent with the bands method approach of treating the electron temperature and density the basic parameters with the radiation field as a non-negligible first order correction.

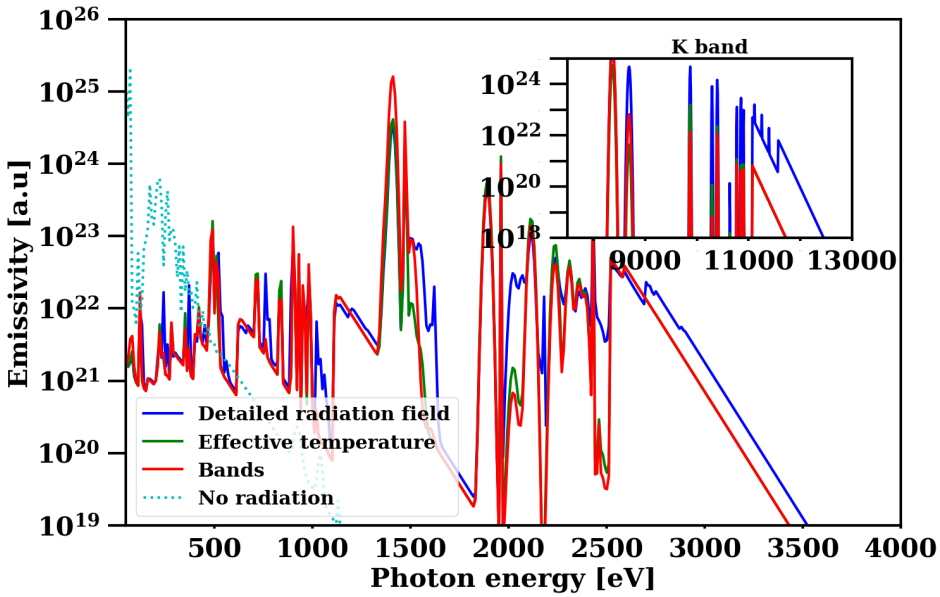

FIG. 12. (Color online) Plasma emission for the third example. Blue: using the full detailed radiation field. Green: using the effective temperature of 428 eV. Red: using the bands method approximation for the radiation field. Dotted Cyan: with no radiation field.

This interpolation method cleanly handles the inclusion of LTE tabulated values obtained with the NLTE code. While those tabulated results are consistent with the full radiation spectrum, only the spectrum in the chosen bands is used for interpolations, guaranteeing continuity of results.

VI. CONCLUSIONS

In this work we have presented the bands method for tabulating NLTE plasma properties. This approximate method is aimed at providing NLTE data within radiation-hydrodynamic simulations which is reasonably consistent with the radiation fields present in such simulations. We have shown in Sec. IV that results using this method are comparable to those from fully detailed calculations for test cases covering a wide range of conditions. We have checked the method for many other cases as well including higher and lower Z materials, with results comparable to the examples presented in this work. The number of active shells, and total number of parameters, should remain manageable even for higher Z materials than we have considered here. For higher Z materials the number of active shells could be higher than the examples presented here, but even in these cases the total number of parameters will remain manageable. It should even be possible to include deep lying shells in cold high Z materials to capture the effect of high energy photons. We have found that in any relevant conditions even with higher Z materials the number of parameters needed for adequately characterizing the radiation field is small enough to allow for tabulation of the results. Moreover, using more parameters for fully characterizing the plasma conditions, e.g. a non thermal electron distribution, is still very much feasible using this method.

As explained in Sec. II the ability to characterize the radiation field with a limited number of parameters addresses several important difficulties. NLTE atomic calculations are a major load on resources in radiation-hydrodynamic simulations. Pre-calculating and tabulating plasma properties from these calculations can dramatically reduce the load on simulations by shifting the computational effort to the one-time construction of the table. This allows the use of more complete atomic models to provide more accurate tabulated data, providing a better match to LTE models used in the same radiation-hydrodynamic simulations. Reducing NLTE calculations in the simulation to a table lookup enables converging NLTE radiation transport calculations with respect to the local radiation field as described in Sec. II.

It is important to emphasize the applicability of this model. Tabulating results with this model requires making several assumptions. The energy distribution of the free electrons is known and can be simply characterized by a limited set of parameters. In the examples presented in this work the electron distribution was assumed to be Maxwellian. It should also be possible to use parameterized electron distributions as in [16] . The atomic properties of the plasma can be calculated in steady state. The identification of the relevant bands is done by calculating the atomic properties without any radiation. It is assumed that adding the radiation does not shift the bands significantly. In the third example of Sec IV we demonstrated a limit of this assumption in the case of a strong radiation fields, where the effective temperature of the radiation is much higher than that of the electrons.

In future work we plan to incorporate the bands method in existing radiation-hydrodynamic codes. For those codes which can use inline NLTE calculations, this will allow direct comparisons with this method and will provide a means to use data

from more accurate atomic models. For codes without the ability to use inline NLTE calculations, this will add the capability to incorporate NLTE physics. In all cases, use of this method will allow a more consistent treatment of radiation transport in NLTE plasma simulations, as is necessary in many current research efforts.

VII. ACKNOWLEDGMENTS

The authors would like to thank Stephanie Hansen, Steve Libby and Mark Foord for many useful discussions regarding this work.

This work was performed under the auspices of the U.S. Department of Energy by LLNS, LLC, under Contract No. DE-AC52-07NA27344. This document was prepared as an account of work sponsored by an agency of the United States government. Neither the United States government nor Lawrence Livermore National Security, LLC, nor any of their employees makes any warranty, expressed or implied, or assumes any legal liability or responsibility for the accuracy, completeness, or usefulness of any information, apparatus, product, or process disclosed, or represents that its use would not infringe privately owned rights. Reference herein to any specific commercial product, process, or service by trade name, trademark, manufacturer, or otherwise does not necessarily constitute or imply its endorsement, recommendation, or favoring by the United States government or Lawrence Livermore National Security, LLC. The views and opinions of authors expressed herein do not necessarily state or reflect those of the United States government or Lawrence Livermore National Security, LLC, and shall not be used for advertising or product endorsement purposes.

[1] H. Chung and R. Lee, High Energy Density Physics **5**, 1 (2009).
[2] Y. Ralchenko, *Modern Methods in Collisional-Radiative Modeling of Plasmas*, Springer Series on Atomic, Optical, and Plasma Physics (Springer International Publishing, 2016).
[3] R. Piron, F. Gilleron, Y. Aglitskiy, H.-K. Chung, C. Fontes, S. Hansen, O. Marchuk, H. Scott, E. Stambulchik, and Y. Ralchenko, High Energy Density Physics **23**, 38 (2017).
[4] S. Hansen, H.-K. Chung, C. Fontes, Y. Ralchenko, H. Scott, and E. Stambulchik, High Energy Density Physics **35**, 100693 (2020).
[5] D. A. Holladay, C. J. Fontes, W. P. Even, and R. G. McClarren, High Energy Density Physics **34**, 100746 (2020).
[6] H. Scott and S. Hansen, High Energy Density Physics **6**, 39 (2010).
[7] M. Rosen, H. Scott, D. Hinkel, E. Williams, D. Callahan, R. Town, L. Divol, P. Michel, W. Kruer, L. Suter, R. London, J. Harte, and G. Zimmerman, High Energy Density Physics **7**, 180 (2011).
[8] G. Kluth, K. D. Humbird, B. K. Spears, J. L. Peterson, H. A. Scott, M. V. Patel, J. Koning, M. Marinak, L. Divol, and C. V. Young, Physics of Plasmas **27**, 052707 (2020).
[9] H. A. Scott, J. A. Harte, M. E. Foord, and D. T. Woods, submitted to Physics of Plasmas (2022).
[10] A. Bar-Shalom, J. Oreg, W. H. Goldstein, D. Shvarts, and A. Zigler, Phys. Rev. A **40**, 3183 (1989).
[11] Y. Frank, E. Louzon, P. Mandelbaum, and Z. Henis, High Energy Density Physics **9**, 594 (2013).
[12] Y. Frank, P. Mandelbaum, and Z. Henis, High Energy Density Physics **12**, 27 (2014).
[13] A. L. Kritcher, D. E. Hinkel, D. A. Callahan, O. A. Hurricane, D. Clark, D. T. Casey, E. L. Dewald, T. R. Dittrich, T. Döppner, M. A. Barrios Garcia, S. Haan, L. F. Berzak Hopkins, O. Jones, O. Landen, T. Ma, N. Meezan, J. L. Milovich, A. E. Pak, H.-S. Park, P. K. Patel, J. Ralph, H. F. Robey, J. D. Salmonson, S. Sepke, B. Spears, P. T. Springer, C. A. Thomas, R. Town, P. M. Celliers, and M. J. Edwards, Physics of Plasmas **23**, 052709 (2016).
[14] I. M. Hall, T. Durmaz, R. C. Mancini, J. E. Bailey, G. A. Rochau, I. E. Golovkin, and J. J. MacFarlane, Physics of Plasmas **21**, 031203 (2014).
[15] D. Hoarty, L. Barringer, C. Vickers, O. Willi, and W. Nazarov, Phys. Rev. Lett. **82**, 3070 (1999).
[16] T. Walton, J. Sebald, I. Golovkin, J. MacFarlane, V. Golovkina, A. Solodov, P. Nilson, and R. Epstein, High Energy Density Physics **35**, 100730 (2020).